Open boundaries in a cellular automaton model for traffic flow with metastable states

Robert Barlovic,[1,*] Torsten Huisinga,[1,†] Andreas Schadschneider,[2,‡] and Michael Schreckenberg[1,§]
[1]*Theoretische Physik Fakultät 4, Gerhard-Mercator-Universität Duisburg, D-47048 Duisburg, Germany*
[2]*Institut für Theoretische Physik, Universität zu Köln, D-50937 Köln, Germany*
(Received 6 June 2002; published 14 October 2002)

The effects of open boundaries in the velocity-dependent randomization (VDR) model, a modified version of the well-known Nagel-Schreckenberg (NaSch) cellular automaton model for traffic flow, are investigated. In contrast to the NaSch model, the VDR model exhibits metastable states and phase separation in a certain density regime. A proper insertion strategy allows us to investigate the whole spectrum of possible system states and the structure of the phase diagram by Monte Carlo simulations. We observe an interesting microscopic structure of the jammed phases, which is different from the one of the NaSch model. For finite systems, the existence of high flow states in a certain parameter regime leads to a special structure of the fundamental diagram measured in the open system. Apart from that, the results are in agreement with an extremal principle for the flow, which has been introduced for models with a unique flow-density relation. Finally, we discuss the application of our findings for a systematic flow optimization. Here some surprising results are obtained, e.g., a restriction of the inflow can lead to an improvement of the total flow through a bottleneck.

DOI: 10.1103/PhysRevE.66.046113 PACS number(s): 89.40.+k, 05.40.−a, 45.70.Vn

I. INTRODUCTION

In recent years, cellular automata (CA) models [1] have attracted a huge attention in statistical physics (and far beyond). The so-called driven lattice gas models, i.e., a lattice connected to particle reservoirs at its boundaries (open boundary conditions) whereby the particles have a preferred hopping direction, are of special interest (see Refs. [2,3] for an overview). The key feature of this class of nonequilibrium models is their simplicity. Albeit the dynamics is based on simple local rules, a rich and nontrivial behavior with a significant relevance to various real world applications [2,3] can be observed. One of the most interesting effects of driven lattice gases are boundary-induced phase transitions [4]. These have been extensively studied so that even exact results exist for some models, e.g., the asymmetric simple exclusion process (ASEP) (see Ref. [3], and references therein). The ASEP has originally been introduced to provide an explanation for the kinetics of protein synthesis [5], but several extensions were proposed to enlarge the potential field of applications. For instance, in Ref. [6] multiple occupation of sites allows us to reproduce the complex dynamics of data transport in the Internet. However, in this paper we will concentrate on driven lattice gases in the context of vehicular traffic flow. Also in this area of transportation theory, generalized ASEPs have been used successfully [7–13].

A few years ago, Nagel and Schreckenberg (NaSch) [14] proposed a probabilistic CA model for traffic flow based on the ASEP. As an extension, velocities $v_{max}>1$ are allowed in the NaSch model with the aim of mimicking effects of acceleration and deceleration. This model is the simplest known CA that can reproduce the basic phenomena encountered in real traffic, e.g., the occurrence of phantom traffic jams [15]. On the other hand, the NaSch model cannot explain all experimental results. Therefore, modifications have been suggested. Here we concentrate on the NaSch model with velocity-dependent randomization (VDR) [16,17], which exhibits metastable states and phase separation between jams and free-flowing vehicles. It is remarkable that, by taking into account further interactions among vehicles on a more detailed level, even empirical single-vehicle data can be reproduced with CA models [18].

So far most studies on CA models for traffic flow were done for systems with periodic boundary conditions. However, open boundaries are relevant for many realistic situations in traffic where the number of vehicles can change, e.g., due to ramps. The special bulk dynamics (with the existence of metastable states and hysteresis) makes the VDR model an interesting candidate for investigating the influence of open boundaries. For models with a *unique* flow-density relation (fundamental diagram), a rather general phenomenological theory of boundary-induced phase transitions was developed in Refs. [4,19–22]. This theory is able to predict the phase diagram of open systems even for complex models. It can be summarized by the extremal principle,

$$J=\begin{cases}\max_{\rho\in[\rho_R,\rho_L]}J(\rho) & \text{for } \rho_L>\rho_R\\ \min_{\rho\in[\rho_L,\rho_R]}J(\rho) & \text{for } \rho_L<\rho_R,\end{cases} \tag{1}$$

which relates the current J in the open system to the fundamental diagram $J(\rho)$ of the periodic system. $\rho_{L/R}$ are the typical densities at the left and right boundaries, respectively. As pointed out in Refs. [23,24], the phase diagram of the NaSch model is similar to the one of the ASEP supporting the predictions of Ref. [19]. Contrary to these results, Cheybany *et al.* [25,26] as well as Huang [27] found large deviations in the phase diagram of the NaSch model in comparison to the ASEP. We will emphasize here (see Sec. III A) that these deviations are related to the special boundary con-

*Email address: barlovic@uni-duisburg.de
†Email address: huisinga@uni-duisburg.de
‡Email address: as@thp.uni-koeln.de
§Email address: schreckenberg@uni-duisburg.de

dition considered, and that the phase diagram of the NaSch model is well comparable to the one of the ASEP.

The fundamental diagram of the VDR model shows a density regime in which the periodic system can be in two different states. One is a metastable homogeneous state and the other one is a phase separated state with a large jam between free-flowing vehicles. Such models with nonunique flow-density relations have not been discussed in the context of the above mentioned phenomenological theory. Therefore it is interesting to analyze which results can be transferred to models with metastability and how many additional effects can be observed due to the metastability. In Ref. [28], a special case of the VDR model (see Sec. II for details), i.e., $v_{max}=1$ and suppressed fluctuations, was studied. An interesting striped microscopic structure appears and the existence of high flow states instead of a maximal current phase, which occurs in the ASEP as well as in the NaSch model under open boundary conditions, are observed. We will show in this paper that these results are transferable to the $v_{max}>1$ case. Furthermore, a phenomenological approach capable of explaining this occurrence of high flow states is given, in good agreement with numerical results. Allowing fluctuations of free-flowing vehicles can lead to interesting effects due to spontaneous jamming. In this context a surprising application will be given, namely, the flow optimization by a systematic reduction of the inflow.

Besides the modeling aspects there is much evidence [24,29] that nonequilibrium phase transitions occur in traffic flow on highways in the vicinity of on and off ramps. From the modeling point of view, such highway segments can be treated as open systems. Hence the understanding of the model dynamics under open boundaries is indispensable in respect to realistic computer simulations of real traffic systems.

II. DEFINITION OF THE MODEL

For the sake of completeness, we will now briefly recall the definition of the VDR model [16,17]. Afterwards, a different insertion strategy is introduced, which is able to eliminate large holes due to hard-core exclusion, occurring when considering the standard insertion procedure,[1] and therefore allowing us to investigate the whole spectrum of possible system states. Throughout the paper we assume that the particles move from left to the right. Particles are therefore inserted at the left end of the chain. The model is defined on a lattice of length L, where every single cell can be empty or occupied by just one particle (vehicle). The speed of each vehicle can take on one of the $v_{max}+1$ allowed integer values $v=0,1,\ldots,v_{max}$. The state of the road at time $t+1$ can be obtained from time step t by applying the following rules to all cars at the same time (parallel dynamics): (1) Step 0: randomization parameter; determination of $p_n=p(v_n)$. (2) Step 1: acceleration; $v_n\rightarrow\min(v_n+1,\ v_{max})$. (3) Step 2: braking; $v_n\rightarrow\min(v_n,\ d_n-1)$. (4) Step 3: randomization;

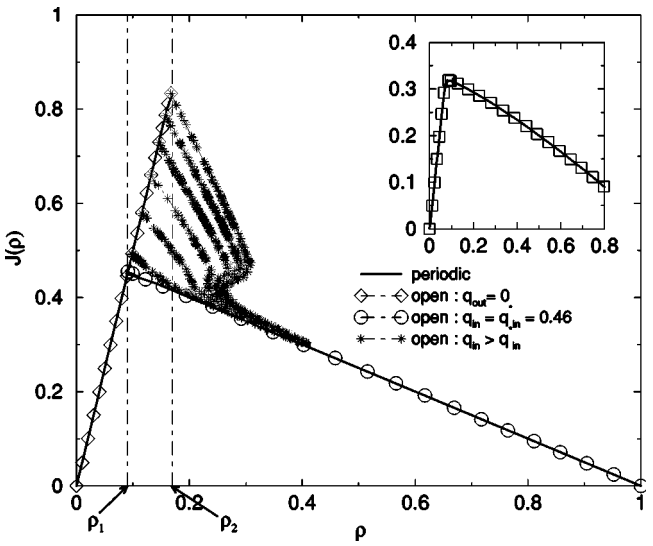

FIG. 1. Fundamental diagram (FD) of the VDR model and the NaSch model (inset). The full lines correspond to periodic boundary conditions while the symbols represent states obtained using open boundaries. The fluctuation parameter is set to $p_0=0.5$ for cars at rest, and $p=0$ for driving cars. In the NaSch model (inset), $p=0.5$ for all velocities. For high inflows ($\star$), the FD shows a very interesting shape, i.e., there are densities where the system can take on three different states.

$$v_n\rightarrow\begin{cases}\max(v_n-1,0) & \text{with probability } p_n,\\ v_n & \text{with probability } 1-p_n,\end{cases}$$

(5) Step 4: driving; $x_n\rightarrow x_n+v_n$.

Here $d_n=x_{n+1}-x_n$ denotes the distance from the next car ahead, where the number d_n-1 of empty cells in front of the nth vehicle is usually called ''headway.'' One time step corresponds to approximately 1 s in real time [14].

For simplicity we study the case with two stochastic parameters only:

$$p(v)=\begin{cases}p_0 & \text{for } v=0\\ p & \text{for } v>0.\end{cases} \tag{2}$$

Here, p_0 controls the fluctuations of cars that have not moved in the previous time step, and thus determines the velocity of a jam. p controls the velocity fluctuations of moving cars. Equation (2) includes the so-called slow-to-start case $p_0\gg p$, where the model shows phase separation and metastable states [16]. It is interesting that an alternative choice of $p(v)$, e.g., $p_0\ll p$ leads to a completely different (even contrary) behavior. Note that for $p_0=p$, the original NaSch model is recovered. For further details on the model, see Ref. [17]. As mentioned before, the special case with $v_{max}=1$ and $p(v=1)=0$ with open boundaries is analyzed in Ref. [28].

In Fig. 1, a typical fundamental diagram of the periodic VDR model (full line) is shown. It can be divided into three different regimes according to the jamming properties [16]. For densities up to ρ_1 no jams appear, and jams existing in the initial conditions dissolve very quickly. Above ρ_2 in con-

[1]Usually, the first cell of the system is occupied with a certain probability.

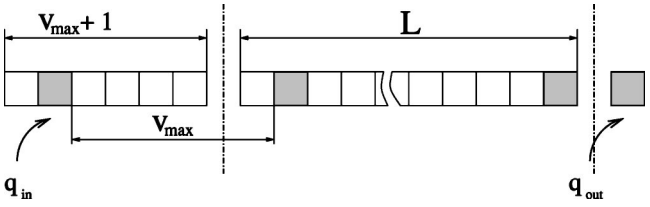

FIG. 2. Schematic representation of the analyzed system. Cars move from left to right, and are represented by dark cells, whereas empty cells are white. The left boundary is given by a small system consisting of $v_{max}+1$ cells. This particle reservoir is occupied by at most one car with probability q_{in}. The right boundary consists of a single cell occupied with probability q_{out}.

trast, no homogeneous state without a jam can exist. This jammed state is characterized by a wide phase separated jam and free-flowing vehicles. However, between the two densities ρ_1 and ρ_2, the system can be in two different states. One is a metastable homogeneous state with a high flow and an extremely long lifetime. Jams can appear due to internal fluctuations or external perturbations, i.e., by stopping cars. The other state is a phase separated state with a wide jam, which can be reached by the decay of the homogeneous state or directly owing to the initial conditions. For large systems, the difference $\rho_2-\rho_1$ strongly decreases and vanishes in the thermodynamic limit. The metastable states of the VDR model are found to be very sensitive against perturbations. In Ref. [30], this sensitivity is studied analytically on the basis of random walk theory. Moreover in Ref. [31], it has been observed that the strong phase separation of the model can be broken by local lattice defects, i.e., stop-and-go traffic that does not occur without lattice defects being found.

A schematic representation of the analyzed system is depicted in Fig. 2. We expanded the width of the left boundary from one single cell to a minisystem of width $v_{max}+1$. This is done to provide a proper insertion strategy allowing us to investigate the whole spectrum of possible system states. That is, the maximum inflow into the system should correspond to the maximum possible flow of the deterministic VDR model.[2] The allocation of the minisystem (left boundary) has to be updated every time step before the vehicles of the complete system. The update procedure consist of two steps. If one cell of the minisystem is occupied, it has to be emptied first. Then a vehicle with initial velocity v_{max} is inserted with probability q_{in}. Its position has to satisfy the following conditions: (i) The headway to the first car in the main system is at least equal to the maximum velocity v_{max}, and (ii) the distance to the main system has to be minimal, i.e., if no vehicle is present in the main system within the first v_{max} cells, the first cell of the boundary is occupied.

We illustrate the benefits of this insertion strategy for the case of the maximum insertion rate $q_{\mathrm{in}}=1$, i.e., in every time step one vehicle with velocity v_{max} is inserted. The initial position of these vehicles will circulate within the boundary from the right to the left end. This is due to the fact that inserted vehicles will occupy a position v_{max} cells ahead, so that the initial position of the next vehicle must be shifted about one cell back to satisfy condition (i). After a while all vehicles move with maximum velocity v_{max} and the minimal headway of v_{max} cells. This corresponds to the maximum flow pattern of the model. For smaller values of q_{in}, the system is adjusted into states with lower densities and flows.

At this point, we want to stress that the maximum flow state of the VDR and NaSch model with $v_{max}>1$, and moreover even a large spectrum of system states cannot be obtained with the help of the standard insertion procedure where just the first cell of the system is occupied with a certain probability. For example, for $q_{\mathrm{in}}=1$ and only one single cell used as boundary, the velocity of inserted cars v_{in} forms a sequence corresponding to a circulating pattern, i.e., $v_{in}=(5,4,3,2,\ldots)$, instead of the circulating positions in the case of the enhanced boundary. As a consequence, one finds an artificial phase diagram and unusual dynamics especially for small p. Further, there is a lack of obtainable system states (high flow) since continuous small gaps cannot be generated within this standard strategy. For details see Refs. [25,26], where the NaSch model $v_{max}>1$ is studied in the context of the standard boundary condition.

The right boundary is realized by a single cell linked to the end of the system. Here the update is applied similar to the case of the left boundary before the general vehicle update procedure. First, the right boundary is cleared (if necessary) and then occupied with probability q_{out}. This corresponds to an outflow probability of $1-q_{\mathrm{out}}$. At last, cars are removed if their velocity is large enough to reach at least the (empty) boundary cell.

Next, an analytical expression for the inflow $J_{free}(q_{\mathrm{in}})$ for the present insertion strategy is given. This expression is valid for all cases investigated in this paper, even for the NaSch model. Note that the inflow into the system is equal to the flow in the free-flow phase. As shown above, the initial position of vehicles circulate from the right end of the boundary to the left end for $q_{\mathrm{in}}=1$. Finally, if the last cell of the boundary is occupied, this vehicle is not able to enter the system anymore, but will move to the first cell within the boundary instead. Therefore, the first cell has to be refreshed in the next update step before a new vehicle may be inserted, so that effectively five cars are inserted in six time steps (for $v_{max}=5$). In general, one has to consider an arbitrary insertion rate q_{in}. Obviously, when calculating the inflow, one has to subtract from the vehicle insertion rate q_{in} just the events that lead to an occupation of the last cell of the boundary. These are all events where $v_{max}+1$ vehicles are inserted consecutively into the boundary. Note, that if a series of insertion events is interrupted (no insertion), the process restarts at the first cell of the boundary. In the language of a stochastic process, this can be formulated as follows. The vehicle insertion can be seen as a sequence of Bernoulli trials, i.e., an insertion of a vehicle corresponds to a ''success'' S (probability q_{in}) while a nonoccupation corresponds to a ''failure'' F (probability $1-q_{\mathrm{in}}$). Now a ''success run'' of length r within a sequence of trials will be defined as follows. A sequence of n letters S and F contains as many

[2]This is also equal to the maximum flow in the deterministic NaSch model. The maximal flows in the stochastic versions of the models are always smaller.

''success runs'' of length r as there are nonoverlapping uninterrupted blocks containing exactly r letters of S each. For example, the sequence $F|SSS|SF|SSS|SSS|SSF$ contains three success runs of length 3. The probability that a success run occurs at the nth trial will be denoted as u_n in the following. Obviously, the probability that a series of r successes occurs at the trials $n, n-1, \ldots, n-r+1$ is equal to $(q_{\mathrm{in}})^r$. In this case the success run occurs at one among these trials.[3] Then the probability that a success run occurs at trial number $n-k (k=0,1,\ldots,r-1)$, and the following k trials are successes is equal to $u_{n-k}(q_{\mathrm{in}})^k$. These events are independent, and one gets the following relation:

$$u_n + u_{n-1} q_{\mathrm{in}} + \cdots + u_{n-r+1}(q_{\mathrm{in}})^{r-1} = (q_{\mathrm{in}})^r, \qquad (3)$$

with $u_1 = u_2 = \cdots = u_{r-1} = 0$. This relation can be solved with the help of a generating function (see Ref. [32] for details). The following solution for the probability that the considered trial corresponds to a success run can be derived:

$$u = \frac{(q_{\mathrm{in}})^r}{1 + \sum_{n=1}^{r-1} (q_{\mathrm{in}})^n} = \frac{(q_{\mathrm{in}})^r}{\sum_{n=0}^{r-1} (q_{\mathrm{in}})^n}. \qquad (4)$$

Returning to the considered boundary with a length of $v_{max}+1$ cells (whereby v_{max} is set to 5), the following expression for the inflow into the system (flow in the free flow phase) is obtained:

$$J_{free}(q_{\mathrm{in}}) = q_{\mathrm{in}} - u = q_{\mathrm{in}} - \frac{q_{\mathrm{in}}^6}{\sum_{n=0}^{5} q_{\mathrm{in}}^n} = \frac{q_{\mathrm{in}}(q_{\mathrm{in}}^5 - 1)}{q_{\mathrm{in}}^6 - 1}. \qquad (5)$$

Note that an analogous analytical expression for the inflow can be used for any v_{max}.

III. SIMULATION RESULTS

Now, the most relevant results of the investigated system are discussed on the basis of numerical simulations. Three different cases of the model dynamics are considered. At first we take a look at the standard NaSch model, which can be viewed as a special case of the VDR model with $p_0 = p$. It provides a point of reference for the cases with metastability and helps to clarify whether the phase diagram of the NaSch model is comparable to the one of the ASEP. Then generic parameter combinations of the VDR model, including slow-to-start behavior and thus metastability, are treated for two different cases. In the first case, fluctuations in the movement of vehicles are suppressed, so that only the jam outflow is stochastic. This case is comparable to the system investigated in Ref. [28], except for the higher velocity $v_{max} > 1$. Moreover, we investigate the case of stochastic vehicle movement such that phase separation is still ensured. For this parameter combination, we point out characteristic additional features due to spontaneous jamming.

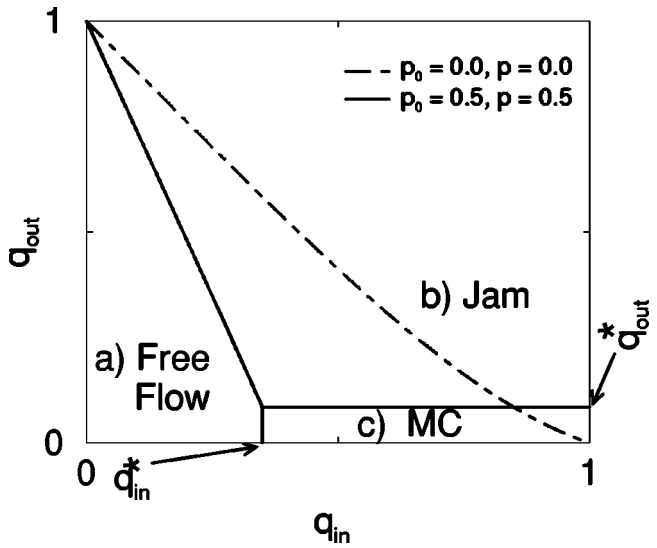

FIG. 3. Phase diagram of the NaSch model derived from Monte Carlo simulations. In the free-flow phase (a) the flow is determined by particle injection at the left boundary, whereas in the jammed phase (b) the particle outflow at the right boundary is the determining factor. On the contrary the flow in the maximum current (MC) phase (c) is given by the maximal possible flow due to the model dynamics. The full lines correspond to the parameter combination $p_0 = p = 0.5$, while the dotted line represents a deterministic system $p_0 = p = 0$. Note that the maximum current phase vanishes for the deterministic case.

A. NaSch model: $p_0 = p$

As already mentioned in Sec. II, the special case $p_0 = p$ of the VDR model is equal to the NaSch model. The corresponding phase diagram obtained by numerical simulations is plotted in Fig. 3 (see also Refs. [23,24]). In the free-flow phase, the system is jam-free except for some small jams formed at the right boundary. Hence the flow is given by the particle inflow. For $v_{max} = 5$, this is equal to $J_{free}(q_{\mathrm{in}}) = q_{\mathrm{in}}(q_{\mathrm{in}}^5 - 1)/(q_{\mathrm{in}}^6 - 1)$ in correspondence with Eq. (5). On the contrary, in the jam phase the system is dominated by large jams of various sizes mostly generated at the right boundary due to the restricted outflow. Consequently, the flow is determined by the outflow parameter q_{out}. On the contrary, in the maximum current (MC) phase, the flow is not restricted by the boundaries but rather by the maximum possible bulk flow of the given model. The MC phase spans a rectangle in the phase diagram. The boundaries are given by the outflow parameter q^*_{out} corresponding to the density in the jam outflow area $\rho_R(q^*_{\mathrm{out}})$, and the probability q^*_{in} according to the maximum flow of the model $[J_{free}(q^*_{\mathrm{in}}) = J_{max}]$. If the inflow $J_{free}(q_{\mathrm{in}})$ surpasses this value, jams are formed most likely direct in front of the boundary, so that the inflow into the system is hindered. Given that the maximum flow in the NaSch model is restricted by the fluctuation parameter, it

[3] One has to take into account here that successes may occur before trial $n-r+1$.

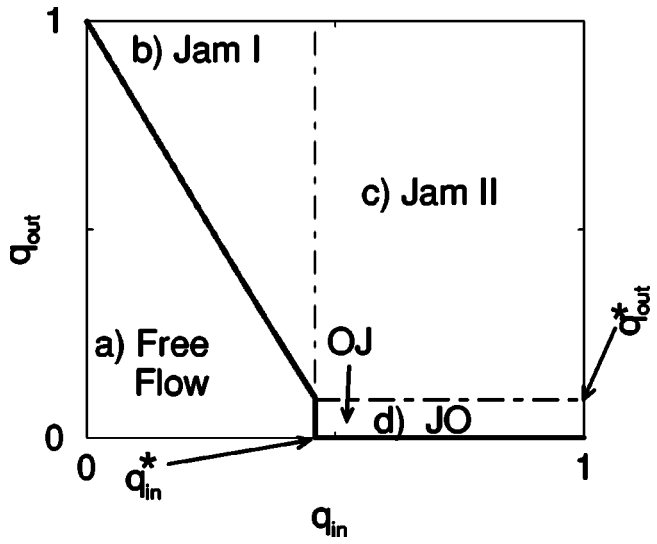

FIG. 4. Phase diagram of the VDR model with deterministic movement ($p=0$) of free-flowing vehicles. The phase diagram is similar to that of the NaSch model. However, there are some differences, most notably on the $q_{\mathrm{out}}=0$ line. Furthermore, two different regions (b) and (c) in the jam phase have to be distinguished with respect to their microscopic structure. The JO phase (d) is characterized by very wide continuously growing jams. In this phase, very high flows can be observed in finite systems.

is clear that the area of the MC phase shrinks with decreasing p until it vanishes completely for the deterministic case $p=0$.

Up to here, the phase diagram of the NaSch model is qualitatively in complete agreement with that of the ASEP ($v_{max}=1$), which is known exactly [33,34]. As already mentioned, this coincides with the argument of Kolomeisky *et al.* [19] that models with one single maximum in the fundamental diagram (periodic system) exhibit the same phases for open boundaries. In order to determine the fundamental diagram from the open system, global flow and densities are measured. These global quantities are obtained by averaging over all cells. In contrast, bulk values are measured in the middle of the system. For low inflow and restricted outflow the bulk density is just ρ_R, whereas for the free-flow case it is given by ρ_L. By varying the inflow q_{in} and the outflow q_{out}, we can generate all possible bulk densities and thus the full fundamental diagram [see Fig. 1 (inset)]. This agrees with that obtained in the periodic system as predicted by the extremal flow principle (1).

We like to stress that another choice of the insertion strategy can produce different phase diagrams. This happens, in fact, for insertion strategies that are not able to achieve the maximum flow of the NaSch model. Then only a part of the state space is scanned.

B. Partially deterministic VDR model: $p_0>0$, $p=0$

We proceed by characterizing the typical properties of the VDR model with metastable states and phase separated large jams. Figure 4 summarizes the results of our Monte Carlo simulations for a VDR model where fluctuations of free-flowing vehicles are suppressed. If not stated otherwise, the stochastic parameter for standing cars is set to $p_0=0.5$ in the following. As in the NaSch model, three different phases can be distinguished. The free-flow phase is very similar to the free-flow phase of the deterministic NaSch model since the vehicles move deterministically through the system. No jams are formed, except for some small ones occurring at the right boundary. However, these small jams dissolve very quickly since the flows in the free-flow phase are smaller than the jam outflow. One very interesting peculiarity that cannot be found in the NaSch model occurs in the case $q_{\mathrm{out}}=0$, i.e., maximal outflow. Here even for inflows greater than the outflow of a jam $J_{free}(q_{\mathrm{in}})>[J_{free}(q^*_{\mathrm{in}})=J_{out}]$, the system is in the free-flow phase. This is indicated by the thick black line in the phase diagram. The origin of this line can be explained quite simply taking into account that vehicles inserted into the system move deterministically, and no perturbations are present. Again the flow within the free-flow phase $J_{free}(q_{\mathrm{in}})$ is given by Eq. (5).

The microscopic structure of the two different jam phases of the VDR model is characterized briefly in the following. A look at typical space-time plots in Fig. 5 reflects that both phases produce a striped structure, i.e., compact jam clusters alternating with free flow regions. At the right boundary, free-flow segments as well as compact clusters are effectively injected into the system. Both regions stay most likely separated due to the dynamics and move backwards. The inflow into a single cluster is produced by the stochastic outflow of the preceding cluster. Therefore the width of the clusters performs a nonbiased random walk [30] until the clusters are far enough from the left boundary, i.e., there is a preceding cluster present. If a cluster finally arrives near the left boundary, it becomes the first one in the system so that its inflow gets equal to the inflow into the system. The cluster width now follows a biased random walk. If the inflow is smaller than the outflow of a jam, $J_{free}(q_{\mathrm{in}})<[J_{free}(q^*_{\mathrm{in}})=J_{out}]$ (jam-I phase), the width decreases in average while it increases for $J_{free}(q_{\mathrm{in}})>[J_{free}(q^*_{\mathrm{in}})=J_{out}]$ (jam-II phase). Note, that in the jam-I phase, the clusters vanish often before they reach the left boundary (Fig. 5, top).

The most interesting result is that a new phase with a nonstationary oscillating density pattern and very high flows in finite systems can be found in the VDR model for $q_{\mathrm{in}}>q^*_{\mathrm{in}}$ and $q_{\mathrm{out}}<q^*_{\mathrm{out}}$. The new phase will be denoted as the jam outflow (JO) phase in the following. This notation is motivated by the fact that in the thermodynamic limit, the system flow is only determined by the JO. Moreover, the microscopic pattern reveals that in the JO phase the system is dominated by one single large jam[4] as can be seen in Fig. 6. This peculiarity has its origin in the metastability of the model, leading to the so-called local-cluster effect [35], i.e., a small local disturbance of the system can lead to the formation of a global wide jam. Due to this effect the global density in the JO phase cannot be related to one of the boundary densities. In fact, the left boundary density (inflow) directly determines the global density and the high flows during the

[4]This is indicated by OJ (one jam) in Fig. 4.

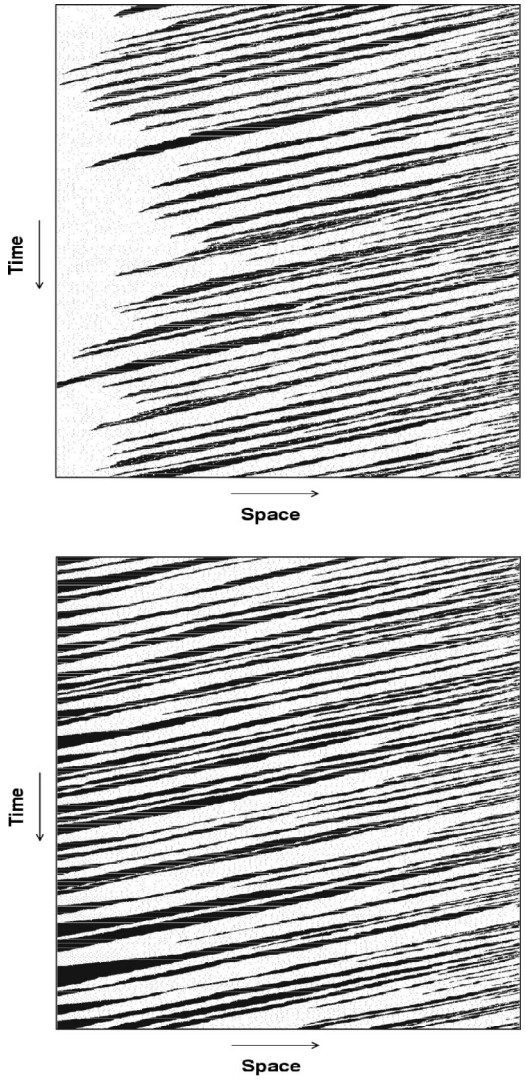

FIG. 5. Typical space-time plots of the two different jam phases of the VDR model for a system consisting of $L=500$ cells. The top part of the figure represents the jam-I phase ($q_{\mathrm{out}}=0.4$, $q_{\mathrm{in}}=0.3$), while the jam-II phase ($q_{\mathrm{out}}=0.4$, $q_{\mathrm{in}}=1.0$) is shown in the bottom plot.

time interval T_{free} (see Fig. 6). On the contrary, the right boundary (outflow) only acts as the local seed that causes the formation of wide global jams. The density within the corresponding jammed time interval T_{jam} depends on the jam outflow, which is a fixed parameter of the model, and the inflow. However, the right boundary density exerts an indirect influence to the global density since it determines the frequency of occurrence for wide global jams. Shortly before the transition to the jam phase, i.e., increasing q_{out}, additional small jams are formed at the right boundary. These small jams constrict the formation of wide global jams so that the global density slightly decreases before it increases again. In fact, this sequence of the density changes (increase-decrease-increase) combined with the high flows are the origin for the interesting shape of the curve ($\star$) corresponding to the JO phase in the FD (see Fig. 1) where the system can take on three different states. Note that in Fig. 1 the global

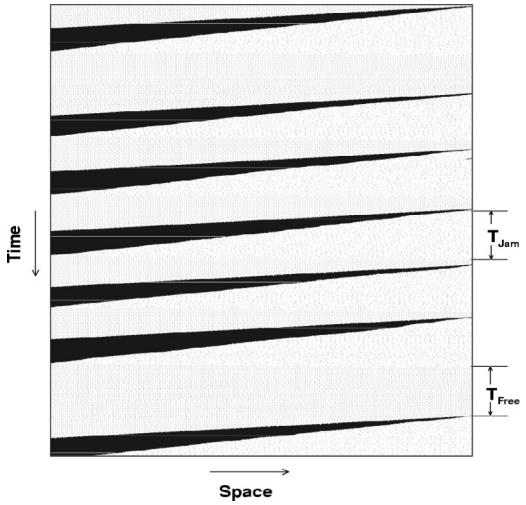

FIG. 6. Space-time plot of the JO phase. The system is dominated by one large jam that does not vanish until it reaches the left boundary. The model parameters are ($p=0.0$, $p_0=0.5$, $q_{\mathrm{out}}=0.01$,$q_{\mathrm{in}}=1.0$) and $L=500$.

densities instead of the bulk densities are considered due to the oscillating density pattern. This may lead to small differences compared to the bulk density in the middle of the system. However, besides the new states that are ascribed to the JO phase ($\star$), the boundaries of the phase diagram can easily be related to the periodic FD of the VDR model if proper parameter combinations are chosen ($\bigcirc$), so that in this sense the extremal current principle is fulfilled.

In the following a phenomenological approach for the flow in the JO phase is given. The jam front that originates from the right boundary moves backwards with a velocity of $v_{jam}=1-p_0$ [17] until it reaches the left boundary. In the meanwhile, i.e., for the time interval T_{jam}, the jam outflow determines the system flow. The duration time T_{jam} is proportional to the system size L. It is the average time interval L/J_{out} needed for the jam front to move from the right to the left boundary plus the time L/v_{max} the last car of the jam needs to move from the left to the right boundary. $J_{out}=v_{max}/[(v_{max}/(1-p_0))+1]$ corresponds to the jam outflow. This leads to $T_{jam}=L[1/J_{out}+1/v_{max}]$ for the mean duration time where the system flow is dominated by the jam outflow. Note that the inflow $J_{free}(q_{\mathrm{in}})$ does not influence this time interval T_{jam} at all. In contrast, the duration T_{free} where the flow is given by the inflow does not depend on the system size, but only on the probability that a jam emerges. Assuming that the right boundary is blocked, the first car in front of it has to slow down if the distance is smaller than the maximum velocity. The probability of finding a car within the scope of v_{max} cells at the blocked boundary is equal to q_{in}. Note that this assumption holds since deterministic movement of free-flowing vehicles is considered so that the inflow at the left boundary can directly be mapped to the right boundary. Thereof only the fraction of about $1/(v_{max}+1)=\frac{1}{6}$ of cars has to brake completely to zero, namely, the cars that are directly in front of the boundary (no more free cell left). This fraction of stopped cars will cause a large jam taking into account that the average flow in the JO phase is

larger than the jam outflow. The rest of the slowed down cars will only brake down to zero (cause a jam) if the boundary is blocked even in the next time step. The probability for this is equal to q_{out}^2. Neglecting the less probable events, one gets the estimation $T_{free}=1/[q_{\mathrm{in}}(\frac{1}{6}q_{\mathrm{out}}+\frac{5}{6}q_{\mathrm{out}}^2)]$ for the time duration that the system flow is determined by the inflow. The flow in the JO phase can then be estimated by

$$J_{JO}=\frac{T_{jam}J_{out}+T_{free}J_{free}}{T_{jam}+T_{free}}. \tag{6}$$

Consequently, the reason for the strong size dependence of the high flow states in the JO phase becomes clear. For small systems, the time periods with a ''high flow'' play an integral part in the overall flow while for larger systems these regions can be more and more neglected. Finally, in the thermodynamic limit only the jam outflow determines the system flow. At this point it should be mentioned that for growing q_{out} even in the jam outflow region (within T_{jam}), additional small jams are formed at the right boundary so that the microscopic structure merges into the striped pattern of the jam phases. As a side effect, these small jams can enlarge the time duration T_{jam}.

The comparison of the predictions for the flow within the JO phase shows good agreement with the simulation results (inset Fig. 7). The top of the figure points out the characteristic properties with respect to the system inflow. The $q_{\mathrm{out}}=0$ line of the phase diagram corresponds to the free flow phase. As soon as the outflow is restricted, i.e., $q_{\mathrm{out}}>0$, the global flow drops to a significantly lower level even for very small $q_{\mathrm{out}}<q_{\mathrm{out}}^*$ (JO phase). Remind that the sharp decline of the flow with growing q_{out} is predicted by the estimation [see Eq. (6) and inset in Fig. 7]. Further, as can be seen in the curve for $q_{\mathrm{out}}=0.01$, for example, the global flow grows with an increasing inflow $J_{free}(q_{\mathrm{in}})$ if very low q_{out} is chosen so that high flow states are present. Obviously this effect is caused by the increased free flow within the time periods T_{free}. However, the flow quickly converges to the jam outflow J_{out} with further increasing q_{out}. If q_{out} trespasses on q_{out}^*, the capacity of the right boundary determines the system flow once the inflow is larger than the capacity of the right boundary. These states can be identified by a large plateau on a level below J_{out} (Fig. 7, top). The system is now in the jam phase. At the bottom of the figure, the dependence between the global flow and the outflow restriction q_{out} is shown. This confirms the results discussed above.

C. Stochastic VDR model: $p_0>p>0$

So far we have considered a particular case of the VDR model where vehicles move deterministically if once started up. A substantial property of this model variant is that the only stochasticity comes from the jam outflow. However, due to the fact that jams are formed only because of the outflow restriction $q_{\mathrm{out}}>0$, the generation of jams within the different phases is determined by the right boundary. Now we investigate the VDR model with stochastic movement of free flowing vehicles as an additional element. We focus on the so-called slow-to-start case with $p_0 \gg p$, for which the expected features as phase separation and metastable states (see Refs. [16,17] for further details) are retained. If not stated otherwise, p_0 is set to 0.5 and p to 0.1. The stochastic movement of vehicles leads to an additional feature, in comparison to the deterministic case, namely, the occurrence of spontaneous jams at sufficiently high flows. A look at the phase diagram (see Fig. 8) reveals strong similarities with the deterministic case. The free-flow phase is not influenced at all by the additional fluctuations, except for some small jams. Moreover, even the two different jam phases are indistinguishable since spontaneous jamming does not play a relevant role within the free-flow segments of the striped jam patterns. In the following, we concentrate our studies on additional effects based on the spontaneous jamming in the JO phase.

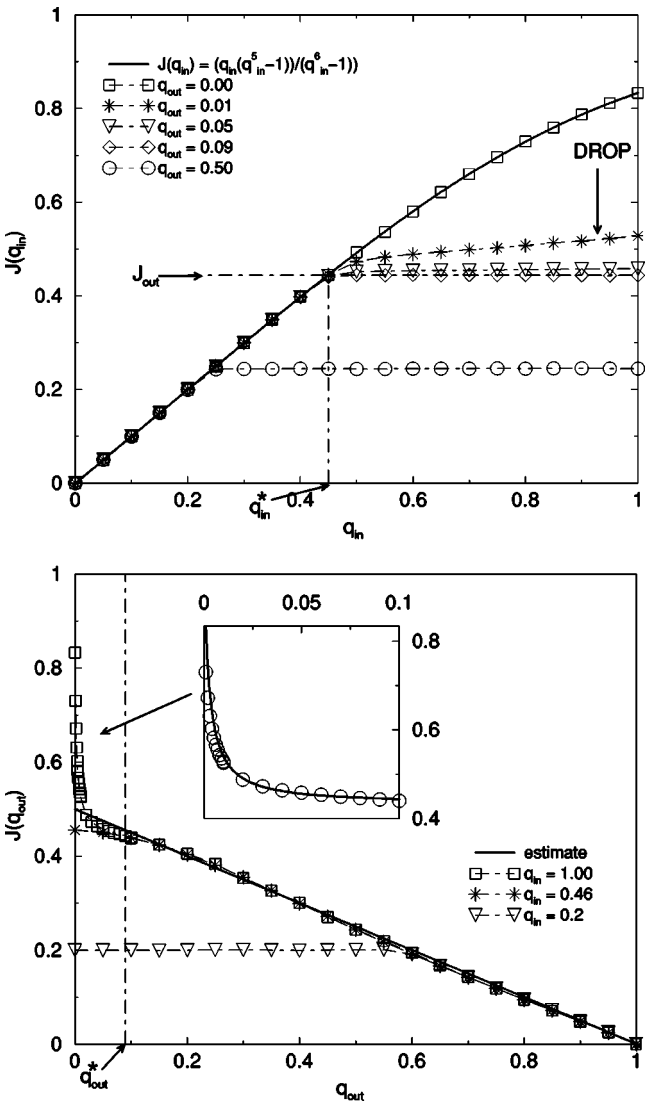

FIG. 7. The dependence between system flow and inflow parameter q_{in} (top), respectively, outflow parameter q_{out} (bottom) is shown for the VDR model with deterministic movement of free-flowing vehicles. The model parameter was chosen as ($L=1000$, $p_0=0.5$, $p=0$).

The most eye-catching difference in comparison to the VDR model with deterministic movement can be seen at the

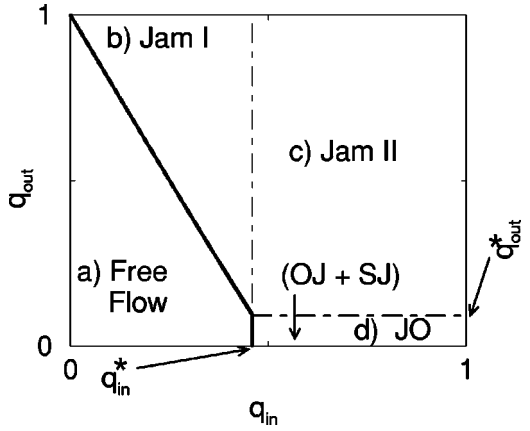

FIG. 8. Phase diagram of the VDR model with stochastic vehicle movement. The phase diagram is very similar to the deterministic case in Fig. 4. However, in contrast, the JO phase has to be distinguished with respect to q_{in}. For relatively small q_{in}, the microscopic pattern is dominated by one large jam marked by OJ (one jam). If larger q_{in} are considered in addition spontaneous jams SJ occur at erratic positions most likely near the left boundary.

top of Fig. 9. The maximum possible flow cannot be achieved for maximum inflow anymore, even for $q_{\mathrm{out}}=0$. On the contrary, the curve corresponding to $q_{\mathrm{out}}=0$ shows a clear maximum at an intermediate inflow. The occurrence of this maximum can be explained as follows. Up to inflows smaller than the outflow of a jam $J_{free}(q_{\mathrm{in}})<[J_{free}(q^*_{\mathrm{in}})=J_{out}]$ the system is in the free-flow phase anyway. Further increasing the inflow shortens the average distance between the vehicles. This enlarges the probability that velocity fluctuations can lead via a chain reaction to the spontaneous formation of a jam. Therefore an increasing inflow leads more and more frequently to spontaneous jams, and finally to decreasing global flows. Note that the sensitivity of the high-flow states also depends on the system size since the probability of finding a vehicle configuration that is capable of producing a jam is proportional to the number of vehicles (see Ref. [17] for details). If the inflow is further increased, the system is overfed and the flow converges into a plateau. Here the global flow is mainly determined by the outflow of jams occurring mostly near the left boundary, but also spontaneously at erratic positions in the system. In addition, if one switches on the outflow restriction $q_{\mathrm{out}}>0$, the occurrence of a separated maximum levels off very fast due to the additional jams generated at the right boundary.

At the bottom of Fig. 9, the dependence of the global flow on q_{out} is plotted. The results are similar to Fig. 7, with the high flow states (inset) occurring when $q_{\mathrm{out}}<q^*_{\mathrm{out}}$. However, while in Fig. 7 the high flow states are most distinct for a maximum inflow $J_{free}(q_{\mathrm{in}}=1)=J_{max}$, here the maximum high flow state is obtained for an optimal q_{in}. That is, if the inflow is too large, the spontaneous jamming levels off the flow drastically, and this greatly reduces the current from the deterministic case.

As a further demonstration of the impact of spontaneous jamming within the JO phase, typical space-time plots for two different inflows are given in Fig. 10. In particular, the interplay among spontaneous jams and jams generated due to

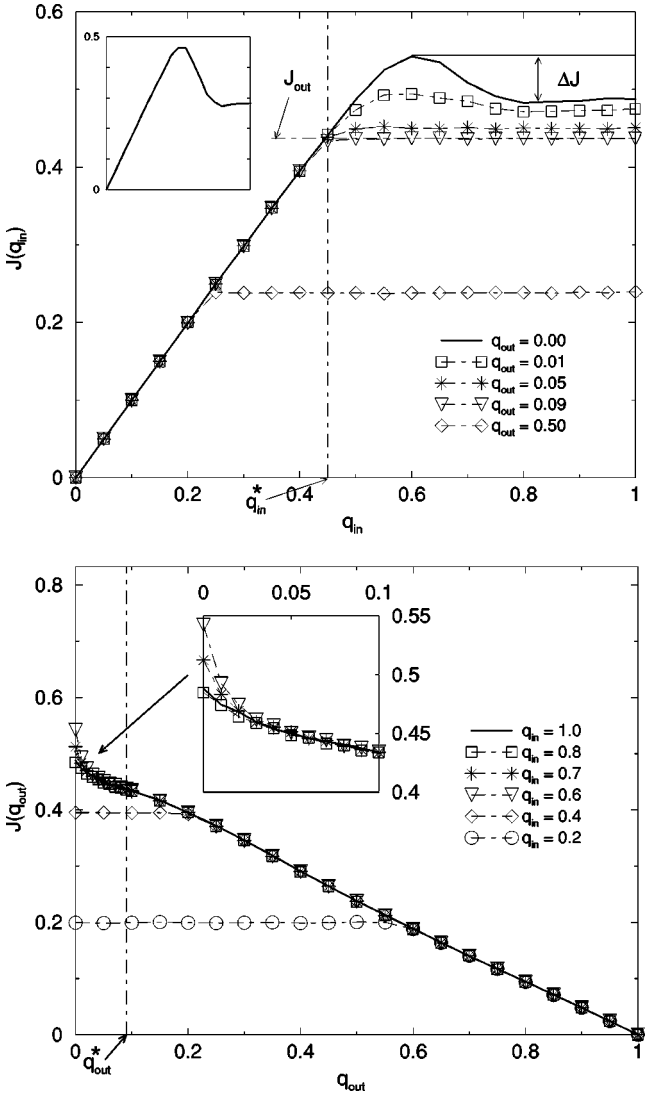

FIG. 9. Top: Global flow vs inflow parameter q_{in}. For $q_{\mathrm{out}}=0$, a wide maximum exists if inflows noticeably smaller than the maximal possible inflow are considered. The maximum vanishes rapidly with increasing q_{in}. Bottom: For capacities (right boundary) above the jam outflow (JO phase $q_{\mathrm{out}}<q^*_{\mathrm{out}}$), high flow states are observable as in the deterministic case, but they are not as distinct. The model parameters are chosen as $p=0.1$, $p_0=0.5$, and $L=1000$.

a restricted outflow is shown. The top of the figure corresponds to a situation with optimal inflow. This means that the inflow into the system is large enough to increase the overall flow due to an increased flow between the time interval of two consecutive large jams. At the bottom of the figure a system with high inflow is depicted. Here spontaneous jams are formed at arbitrary positions mostly near the left boundary caused by fluctuations in addition to the large jams generated due to the outflow restriction. Consequently, the system flow is then completely determined by the jam outflow. This is very undesirable since the corresponding global flows are considerably lower then for an optimal situation. In this context in the following we show how to optimize the overall flow systematically by regulating the inflow into a system

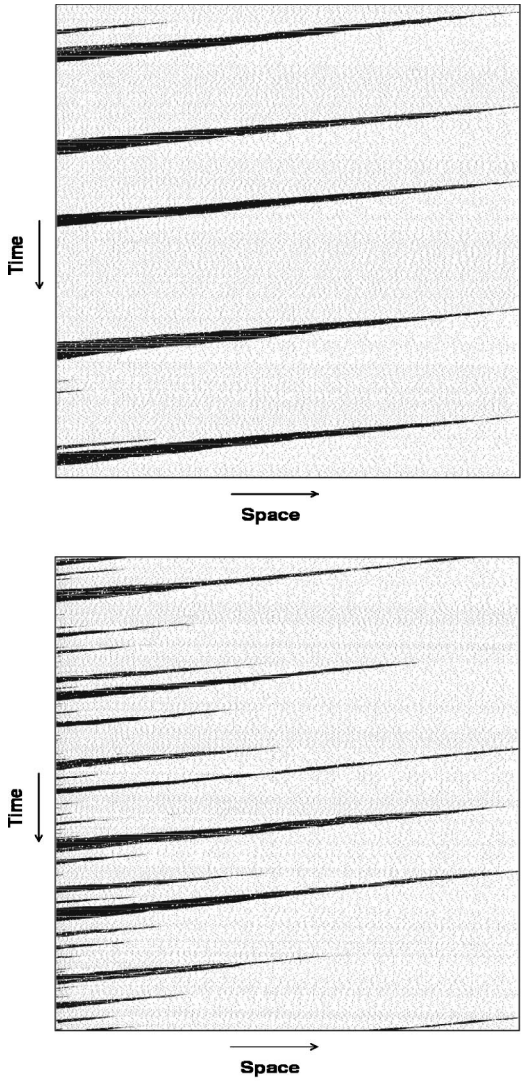

FIG. 10. Typical space-time plots of the two distinguishable states in the JO phase. The parameters are ($q_{\mathrm{out}}=0.01$, $L=500$, $T=10\,000$, $p=0.1$, $p_0=0.5$), with $q_{\mathrm{in}}=0.65$ for the top part and $q_{\mathrm{in}}=1.0$ for the bottom one.

and therewith suppressing the emergence of spontaneous jams.

D. Application: Flow optimization

Besides the theoretical interest in metastable states, there are also interesting real world traffic applications for this phenomenon. The previous discussion about the existence of high flow states shows that one can optimize the throughput if the homogeneous state is stabilized by controlling the inflow into the system. This strategy was followed, for example, in minimizing frequent jams in the Lincoln and the Holland tunnels in New York [36,37]. Before traffic lights were installed, jams used to form spontaneously within the tunnel. The installed traffic lights at the entrance restrict the inflow so that a critical value cannot be exceeded anymore. With this strategy a remarkable increase of the overall capacity was achieved. The modeling aspect of this situation can

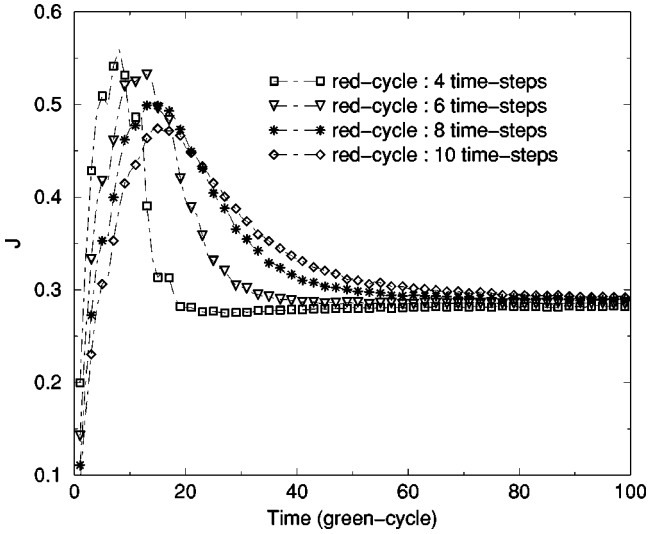

FIG. 11. The global flow is plotted vs the green cycle time for some red cycle times. Obviously, the flow is nearly twice as high for the optimal parameter combination than for a system without inflow restriction. The limit of large green cycle times corresponds to an unrestricted system. Note that we have chosen $p_0=0.75$ to stress the strong impact of the inflow restriction onto the overall flow. The remaining model parameters are chosen as follows: $p=0$, $q_{\mathrm{in}}=1.0$, $q_{\mathrm{out}}=0.0$, $L=1000$.

be seen within the framework of this paper. The inflow $J_{free}(q_{\mathrm{in}})$ represents the traffic demand. If a very high q_{in} is allowed, this typically leads to spontaneous jams inside the ''tunnel'' as explained in the previous sections.

In Fig. 11, a situation is depicted where a traffic light is implemented in the simulations. The inflow is set to the maximum possible value $J_{free}(q_{\mathrm{in}}=1)=J_{max}$ to guarantee that an uncontrolled inflow generates a multitude of jams. The traffic light itself is implemented in such a way that the connecting cell between the system and the left boundary is blocked for the duration of the red-signal time period and open for the green-signal period. As one can see in Fig. 11, for an optimal signal combination the possible flow is about twice as high as for an unrestricted system. In reality, i.e., the case of the Lincoln and Holland tunnels, improvements of about 20% have been achieved. Note that in the case of large green-signal periods the system converges to a system without traffic light restriction. However, the flow in the JO phase for $q_{\mathrm{in}}=1$ is determined by the jam outflow that can easily be adjusted by p_0. Therefore the choice of p_0 determines the possible gain achieved by the flow optimization strategy so that the model can simply be calibrated to real traffic conditions.

IV. CONCLUSIONS

We have analyzed the VDR model that enhances the well-known Nagel-Schreckenberg cellular automata model for traffic flow with features such as phase separation and metastable high flow states. In our investigation we focused on the effects of open boundary conditions. For this purpose we have defined an insertion strategy that allows us to analyze the complete phase diagram of the model. A further advan-

tage of this insertion scheme is that the corresponding inflow into the system can be determined by an analytical approach.

As a special case of the VDR model we also study the behavior of the NaSch model under open boundaries since less is known about this model for $v_{max}>1$. It is shown that the phase diagram of the NaSch model for $v_{max}=5$ is qualitatively in total agreement with that of the ASEP. This once more confirms the recent prediction by Kolomeisky *et al.* [19] that models with a unique flow-density relation, and one single maximum in the fundamental diagram of the periodic system should show a comparable phase diagram that is governed by an extremal current principle. Moreover, it is shown that an unsuitable choice of the insertion strategy might lead to a different phase diagram where one or even more phases are missing.

The main focus of this paper is on the VDR model with slow-to-start behavior. This exhibits phase separation and metastable high flow states, and the corresponding periodic system has a nonunique flow-density relation in a certain density regime. In this work we make clear how far the results from the NaSch model can be transferred and what additional effects can be found due to the more complex fundamental diagram.

First we studied a slow-to-start case where fluctuations of free-flowing vehicles are suppressed, so that the only stochasticity is found in the boundaries and the jam outflow. The jammed phases of this model variant consist of a very characteristic microscopic structure. We found a striped pattern with alternating large jam clusters and free-flow segments. It appears as if the microscopic structure of the jammed phases is generic for driven lattice gases with metastability. For example, in Ref. [28] a very similar microscopic structure has been observed in a related model. Furthermore, in the area that corresponds to the maximum current (MC) phase of the NaSch model, a phase denoted as JO (jam outflow) phase can be observed in the VDR model. This phase can be seen besides the striped microscopic jam patterns as a signature of metastability. For very low q_{out} (outflow restriction), very high flows are observed in a finite system in this phase. The corresponding microscopic structure reveals that the system is then dominated mainly by a single large jam that originates from the right boundary (outflow restriction) and grows rapidly since the inflow into the jam, which is determined by the system inflow, is larger than the outflow of a jam. The explanation for the high flows within this phase is given by jam-free areas between two succeeding large jams. Since the only seed for jamming is found in the restricted outflow, a finite probability that the system is jam-free for a certain time exists. In these jam-free areas, the high inflow contributes a significant portion to the overall flow. However, this portion decreases with increasing system sizes, and in the thermodynamic limit the flow is determined by the jam outflow. For growing q_{out} even within the JO phase, additional small jams are formed at the right boundary and the microscopic structure transforms into the striped pattern of the jam phase. The flow in the thermodynamic limit is given by the jam outflow, which then corresponds to the maximum flow. This may be seen as a link between the MC phase of the NaSch model and the JO phase of the VDR model. Due to the fact that the metastable branch of the VDR model vanishes in the thermodynamic limit, the fundamental diagram gets the same simple structure containing one single maximum as the one of the NaSch model. The only difference is the fact that the maximum flow in the VDR model corresponds to the jam outflow while the maximum flow of the NaSch model is marginally larger than the jam outflow [38] since in the NaSch model spontaneous jams can occur even in the jam outflow area. Nevertheless, the prediction of Ref. [19] for models with one single maximum holds even for the VDR model in the thermodynamic limit except for $q_{\mathrm{out}}=0$. Further, a simple phenomenological approach has been suggested for the flow in the JO phase that shows good agreement with numerical data and confirms that the approach of an interplay between jam-free segments and large jams holds.

We have also investigated the VDR model with stochastic movement of cars concentrating on the slow-to-start case with $p_0 \gg p$. This exhibits the expected features such as phase separation and metastable states. The stochastic movement of vehicles leads to an additional feature that is the occurrence of spontaneous jams at sufficiently high inflows. However, this effect neither plays an important role in the ''free-flow'' phase nor in the jam phases which are nearly unaffected, and therefore are equal to the phases of the deterministic version. But the spontaneous jamming is a significant feature in the JO phase. For low q_{out}, it is shown that the maximum possible flow is no more achieved as in the deterministic case for a maximum inflow, but rather for intermediate inflows. This can be explained by the sensitivity of the metastable high flow states, which increases with increasing inflows. In other words, the higher the inflow into the system, the more frequently spontaneous jams appear which influence due to a reduced jam outflow the overall flow drastically. As an interesting application to real traffic, it is further shown how the overall flow can be optimized systematically by the installation of a traffic light regulating the inflow into the system and thereby suppressing the formation of spontaneous jams.

Similar results [39] can be found in a continuum version of the NaSch model, the SK model [40]. This model also implicitly contains slow-to-start behavior. There is, however, an important difference from the VDR model since the high flow states in the metastable region of the SK model seem to be much more stable than those of the VDR model [41].

Summarizing, the results presented here are of theoretical and practical relevance for various applications of traffic flow. Due to their simplicity, cellular automata models have become quite popular in recent years, which makes a proper understanding of the underlying models indispensable. In particular, from the theoretical point of view several interesting points are the focus of this work. It is shown that for a proper insertion strategy, the phase diagram of the NaSch model is equivalent to that of the ASEP. In this connection the origin of contradictory results is discussed. Further, it is shown that a striped microscopic jam pattern within the jam phases seems to be generic for models with metastability. As another typical feature of the analyzed model, a phase where metastable high flow states can exist in finite systems

is observed. This phase can be related to the maximum current phase of the NaSch model. It is shown how the high flow states are influenced by the restricted outflow, which can lead to wide jams, and by spontaneous jamming. From a practical point of view a flow optimization strategy applied, for example, in the Lincoln and the Holland tunnels in New York is reproduced with the help of the finite-size effects occurring in the analyzed model.

[1] S. Wolfram, *Theory and Applications of Cellular Automata* (World Scientific, Singapore, 1986).

[2] B. Schmittmann and R. K. P. Zia, in *Phase Transitions and Critical Phenomena*, edited by C. Domb and J. L. Lebowitz (Academic Press, New York, 1995), Vol. 17.

[3] G. M. Schütz, in *Phase Transitions and Critical Phenomena*, edited by C. Domb and J. L. Lebowitz (Academic Press, New York, 2000), Vol. 19.

[4] J. Krug, Phys. Rev. Lett. **67**, 1882 (1991).

[5] J.T. MacDonald and J.H. Gibbs, Biopolymers **7**, 707 (1969).

[6] T. Huisinga, R. Barlovic, W. Knospe, A. Schadschneider, and M. Schreckenberg, Physica A **294**, 249 (2001).

[7] *Traffic and Granular Flow*, edited by D. E. Wolf, M. Schreckenberg, and A. Bachem (World Scientific, Singapore, 1996).

[8] *Traffic and Granular Flow '97*, edited by M. Schreckenberg and D. E. Wolf (Springer, New York, 1998).

[9] *Traffic and Granular Flow '99*, edited by D. Helbing, H. J. Herrmann, M. Schreckenberg, and D. E. Wolf (Springer, New York, 2000).

[10] I. Prigogine and R. Herman, *Kinetic Theory of Vehicular Traffic* (Elsevier, Amsterdam, 1971).

[11] C.F. Daganzo, M.J. Cassidy, and R.L. Bertini, Transp. Res., Part A: Policy Pract. **33A**, 365 (1999).

[12] D. Chowdhury, L. Santen, and A. Schadschneider, Phys. Rep. **329**, 199 (2000).

[13] D. Helbing, Rev. Mod. Phys. **73**, 1067 (2001).

[14] K. Nagel and M. Schreckenberg, J. Phys. I **2**, 2221 (1992).

[15] M. Schreckenberg, A. Schadschneider, K. Nagel, and N. Ito, Phys. Rev. E **51**, 2939 (1995).

[16] R. Barlovic, L. Santen, A. Schadschneider, and M. Schreckenberg, Eur. Phys. J. B **5**, 793 (1998).

[17] R. Barlovic, Diploma thesis, Universität Duisburg, 1998.

[18] W. Knospe, L. Santen, A. Schadschneider, and M. Schreckenberg, J. Phys. A **33**, 48477 (2000).

[19] A.B. Kolomeisky, G.M. Schütz, E.B. Kolomeisky, and J.P. Straley, J. Phys. A **31**, 6911 (1998).

[20] V. Popkov and G.M. Schütz, Europhys. Lett. **48**, 257 (1999).

[21] T. Antal and G.M. Schütz, Phys. Rev. E **62**, 83 (2000).

[22] J.S. Hager, J. Krug, V. Popkov, and G.M. Schütz, Phys. Rev. E **63**, 056110 (2001).

[23] L. Santen, doctoral thesis, Universität zu Köln, 1999.

[24] V. Popkov, L. Santen, A. Schadschneider, and G.M. Schütz, J. Phys. A **34**, L45 (2001).

[25] S. Cheybani, J. Kertesz, and M. Schreckenberg, Phys. Rev. E **63**, 016107 (2001).

[26] S. Cheybani, J. Kertesz, and M. Schreckenberg, Phys. Rev. E **63**, 016108 (2001).

[27] D.W. Huang, Phys. Rev. E **64**, 036108 (2001).

[28] C. Appert and L. Santen, Phys. Rev. Lett. **86**, 2498 (2001).

[29] L. Neubert, L. Santen, A. Schadschneider, and M. Schreckenberg, Phys. Rev. E **60**, 6480 (1999).

[30] R. Barlovic, A. Schadschneider, and M. Schreckenberg, Physica A **294**, 525 (2001).

[31] A. Pottmeier, R. Barlovic, W. Knospe, A. Schadschneider, and M. Schreckenberg, Physica A **308**, 471 (2002).

[32] W. Feller, *An Introduction to Probability Theory and Its Applications* (Wiley, New York, 1968), Vol. I.

[33] M.R. Evans, E.R. Speer, and N. Rajewsky, J. Stat. Phys. **95**, 45 (1999).

[34] J. de Gier and B. Nienhuis, Phys. Rev. E **59**, 4899 (1999).

[35] B.S. Kerner and P. Konhäuser, Phys. Rev. E **50**, 54 (1994).

[36] H. Greenberg and A. Daou, Oper. Res. **8**, 524 (1960).

[37] R. Herman and K. Gardels, Sci. Am. **6**, 35 (1963).

[38] B. Eisenblätter, L. Santen, A. Schadschneider, and M. Schreckenberg, Phys. Rev. E **57**, 1309 (1998).

[39] A. Namazi, N. Eissfeldt, P. Wagner, and A. Schadschneider (unpublished).

[40] S. Krauß , P. Wagner, and C. Gawron, Phys. Rev. E **54**, 3707 (1996); **55**, 5597 (1997).

[41] K. Nagel, C. Kayatz, and P. Wagner, *Traffic and Granular Flow '01* (Springer, New York, in press).